

Self-Aggregation of Synthetic Zinc Chlorins with a Chiral 1-Hydroxyethyl Group as a Model for *in vivo* Epimeric Bacteriochlorophyll-*c* and *d* Aggregates

Hitoshi Tamiaki*, Shoichiro Takeuchi, Seiichi Tsudzuki, Tomohiro Miyatake
and Rikuhei Tanikaga

Department of Bioscience and Biotechnology, Faculty of Science and Engineering, Ritsumeikan University,
Kusatsu, Shiga 525-8577, Japan

Received 19 February 1998; accepted 13 April 1998

Abstract: 3¹-Epimerically pure zinc 3-(1-hydroxyethyl)-13¹-oxochlorins possessing several substituents at the 20-position were prepared. In non-polar organic solvents, the synthetic zinc complexes self-aggregated to form oligomers with >700-nm absorption and giant CD peaks, which were dependent upon the 3¹-absolute configuration as well as the 20-substituents. The *in vitro* self-aggregates of each epimeric zinc chlorin with a 20-methyl group showed similar visible and CD spectra with the *in vivo* bacteriochlorophyll-*c* (3¹*R/S*=2/1) aggregates in extramembranous antennae of a green photosynthetic bacterium. The spontaneous *in vitro* self-aggregates of 3¹*R/S*(=2/1)-epimeric mixture of the zinc 20-methylchlorins were different from the natural supramolecules, indicating that *in vivo* slow oligomerization of 3¹*R/S*(=2/1)-bacteriochlorophylls-*c* induced the regular supramolecular structures and/or the epimerically separated assemblies. © 1998 Elsevier Science Ltd. All rights reserved.

INTRODUCTION

Green photosynthetic bacteria have unique light-harvesting antenna systems (=chlorosomes). In natural chlorosomes, major chlorophyllous pigments self-aggregate to form oligomers which are characteristic of red-shifted absorption bands compared with the corresponding monomers.¹ The pigments are several homologues of magnesium complexes of 3¹-hydroxy-13¹-oxochlorins (=bacteriochlorophyll(=BChl)s-*c* and *d*, see Chart 1). BChls-*c* and *d* represent 20-methyl (R²⁰=Me) and 20-unsubstituted compounds (R²⁰=H), respectively. Natural BChls-*c/d* have a variety of substituents (=C_nH_m) at the 8- and 12-positions (R⁸ and R¹²) as well as the ester chain on the 17-propionate (R). The variation of the substituents affects the supramolecular structures of the self-aggregates and also energy migration in the oligomer. Several reports supported such controls in natural and model systems.² On the other hand, the absolute configuration at the chiral 3¹-position in the 3-(1-hydroxyethyl) group is dependent upon the bacteria species: typically BChl-*c* of a green filamentous gliding (non-sulfur) bacterium (Chloroflexaceae), *Chloroflexus aurantiacus* is a 2:1 mixture of 3¹*R*- and 3¹*S*-epimers.³

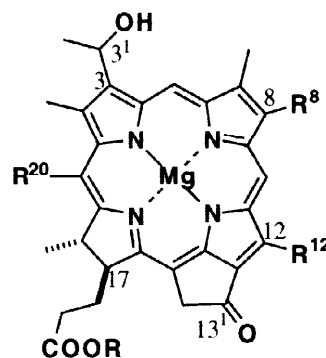


Chart 1. Chlorosomal chlorophylls
BChl-*c*: R²⁰=Me
BChl-*d*: R²⁰=H

Recently, the diastereomeric control of the *in vitro* self-aggregates was reported: $3^1R/S$ epimerically pure samples gave different aggregates in organic solvents.⁴ We know of few works^{4e,f} which tried to elucidate the reasons why the 3^1 -epimeric mixtures are in natural systems.

We reported earlier that synthetic zinc 3-hydroxymethyl-13¹-oxochlorins are good (stable and available) models for natural BChls-*c/d*.^{5–7} Here we report on the synthesis of 3^1 -epimerically pure zinc 3-(1-hydroxyethyl)-13¹-oxochlorins **3** and the self-aggregation of the 3^1 -epimeric mixtures (several ratios, $3^1R/3^1S = 1/0 - 0/1$) in non-polar organic solvents.

RESULTS AND DISCUSSION

Synthesis of Zinc Chlorins

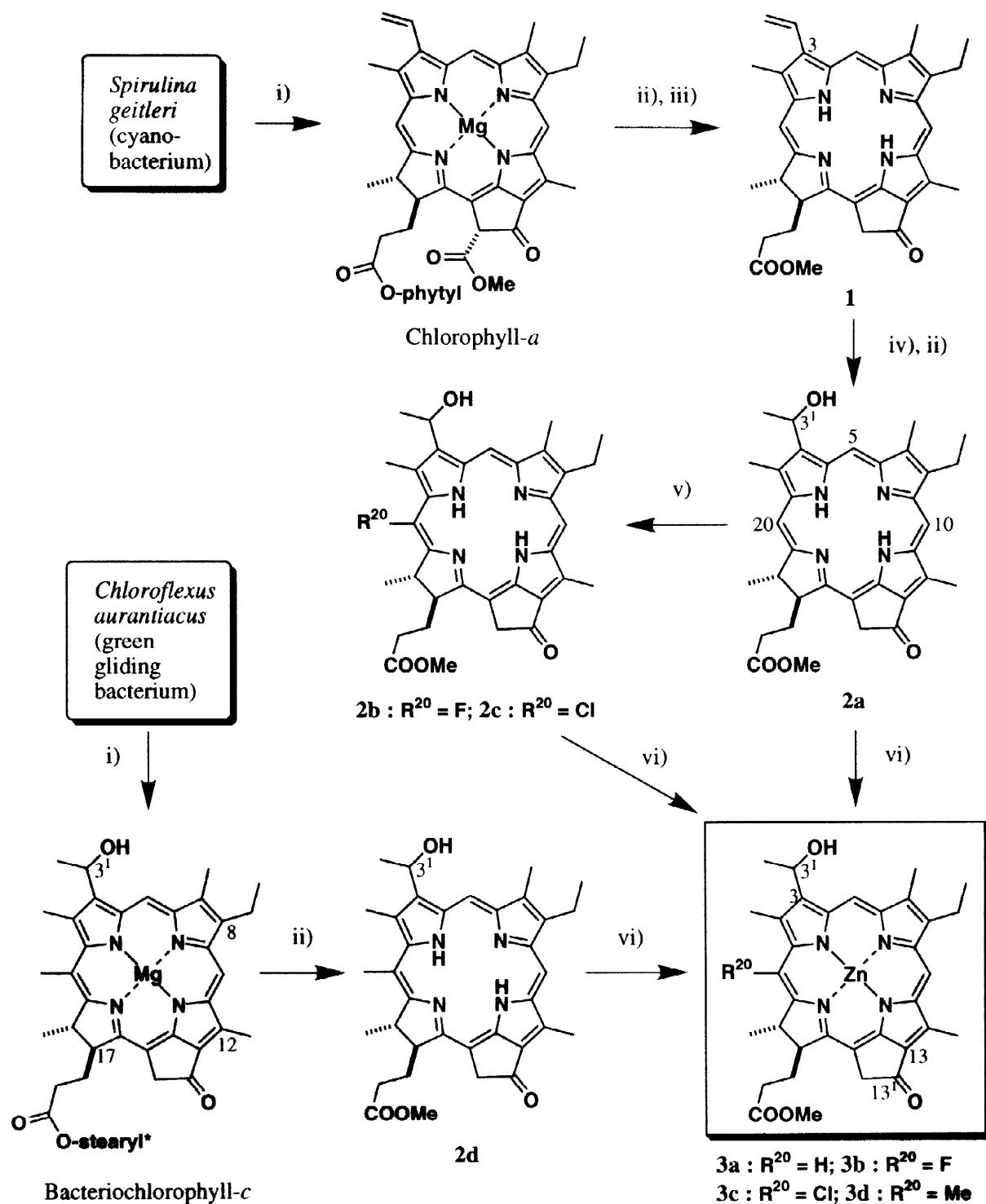
Chlorophyll(=Chl)-*a* was extracted from a cyanobacterium, *Spirulina geitleri* (see Scheme 1).⁵ The commercially available species (used as carp feed, Dainippon Ink and Chemicals) has only Chl-*a* as a chlorophyllous pigment and Chl-*a* in the dry cell was more easily separated from other pigments than in higher plants (e.g., spinach) containing Chl-*b*. After treatment of the cell extract mixture by sulfuric acid in methanol, crude methyl pheophorbide-*a* was obtained by recrystallization from methanol and successive washing with water and hexane. The black solid was pyrolyzed and column chromatography and recrystallization gave pure methyl pyropheophorbide-*a* (**1**).⁵ Hydration of the 3-vinyl group afforded methyl bacteriopheophorbide-*d* (**2a**) by slight modification of procedures originally reported by Smith and his colleagues (see Experimental section).⁸ The reaction occurred non-diastereoselectively to lead an epimeric mixture of 3^1R (**2aR**) / 3^1S (**2aS**) = 1 / 1 (from ¹H-NMR spectral analysis). 20-Unsubstituted chlorin **2a** was halogenated according to our previous report⁶ to give 20-fluoro / 20-chlorochlorins **2b** ($R^{20}=F$) and **2c** ($R^{20}=Cl$).

BChl-*c* was extracted from a green non-sulfur bacterium, *Chloroflexus aurantiacus* (see Scheme 1). The cultured species has only one homologue of BChl-*c* possessing ethyl and methyl groups at the 8- and 12-positions, respectively, except for a variation of 17-propionate ester chains and 3^1 -chirality,³ while green sulfur bacteria have many homologues possessing several alkyl groups at the 8- and 12-positions. The extracted BChl-*c* was changed to methyl ester of metal-free chlorin **2d**. The formula corresponds to 20-methylation of **2a**. Methyl bacteriopheophorbide-*c* (**2d**) prepared was an epimeric mixture of 3^1R (**2dR**) / 3^1S (**2dS**) = 2 / 1 because naturally occurring BChl-*c* in the chlorosome is an epimeric mixture of the same ratio.

The metal-free chlorins **2a-d** were metallated to give zinc complexes **3a-d**. Purification of flash column chromatography (FCC), recrystallization and HPLC (only MeOH as an eluant) gave 3^1 -epimeric mixtures of pure zinc chlorins. All the synthetic chlorins were characterized by ¹H-NMR (1D and 2D-COSY/NOESY), visible and mass spectra.

Separation of Epimeric Chlorins

3^1 -Epimeric mixtures of metal-free chlorins **2a** and **2d** have already been separated by several runs of reversed-phase HPLC (achieved upon recycling).⁸ We also tried to separate the mixtures of all synthetic metal-free chlorins **2a-d** but were able to get only poorly separated chromatograms by a single run of HPLC.⁹ However, an epimeric mixture (1:1) of zinc complex **3a** was easily separated by the single run (see Scheme 2). Under the same conditions (Cosmosil 5C₁₈-AR, 4.6 φ × 250 mm, Nacalai Tesque, CH₃OH / H₂O = 4 / 1, 1.0



Scheme 1. Synthesis of zinc chlorins 3

i) extraction; ii) H₂SO₄/MeOH; iii) collidine-reflux; iv) HBr/AcOH; v) C₅H₅NF⁺CF₃SO₄⁻/CH₂Cl₂–C₆H₅CH₃–CH₃CN for fluorination, NaClO₂/H₂O–THF for chlorination; vi) Zn(OAc)₂/MeOH–CH₂Cl₂.

* including other esters.³

mL / min), 3¹-epimeric bands were completely separated (see Experimental section) and the separation ratio (R_s) between bands of (3¹*R*)-**3R** and (3¹*S*)-**3S** increased with 20-substitution: $R_s = 1.9$ (**3a**, R²⁰=H) < 2.6 (**3b**, R²⁰=F) < 2.9 (**3c**, R²⁰=Cl) < 3.0 (**3d**, R²⁰=Me). After preparative HPLC separation of the epimeric mixture of **3a**, each fraction was dried *in vacuo*. The separated zinc chlorins (**3aR** / **3aS**) were demetallated by the action of acid to give 3¹-enantiomerically pure chlorins (**2aR** / **2aS**) without epimerization at the 3¹-position (see Scheme 2).¹⁰ Each metal-free chlorin in chloroform-*d* was analyzed by ¹H-NMR. Compared with reported chemical shifts at the *meso*-positions (5-, 10-, 20-H) of each stereochemistry-determined **2a**,⁸ the metal-free chlorin derived from the first and second fractions was **2aR** and **2aS**, respectively, and then the first eluted band (retention time, *rt* = 32 min) was assigned to (3¹*R*)-**3aR** and the second band of *rt* = 34 min was (3¹*S*)-**3aS**.

Epimerically pure chlorins **2aR** / **2aS** were fluorinated in an analytical scale (< 1 mg) and successively zinc-metallated as described above to afford epimeric zinc 20-fluorochlorins **3bR** / **3bS** without epimerization, respectively. Each zinc chlorin was analyzed with HPLC, indicating that the first band (*rt* = 34 min) was **3bR** and the second band (*rt* = 39 min) was **3bS**. Moreover, in a preparative scale (> 10 mg), 20-unsubstituted chlorin **2aR** (or **2aS**) was fluorinated (*vide supra*) to give epimeric 20-fluorochlorin **2bR** (or **2bS**) stereoselectively and the first (or second) eluted band in HPLC of zinc fluorochlorin **3b** was demetallated to give epimerically pure **2b**. Comparison of the two ¹H-NMR spectra of the produced metal-free 20-fluorochlorins led to the same assignment as in HPLC analysis. Similarly, metal-free 20-unsubstituted chlorins **2aR** / **2aS** were converted to zinc 20-chlorochlorins **3cR** / **3cS** by chlorination and zinc-metallation. HPLC analysis showed that the first (*rt* = 31 min) and second bands (*rt* = 37 min) were **3cR** and **3cS**, respectively. Identification of ¹H-NMR spectra of **2cR** (or **2cS**) from chlorination of **2aR** (or **2aS**) with epimerically pure **2c** from demetallation of the first (or second) HPLC fraction of **3c** also supported the assignment derived from HPLC analysis.

Zinc methyl bacteriopheophorbide-*c* was a 2 : 1 mixture of **3dR** / **3dS** as mentioned above. HPLC of the mixture gave the chromatogram that the 26-min band was 2-fold larger than the 29-min band. Therefore, the first eluted band was **3dR** and the second was **3dS**. In all four HPLC separations described here, the first fraction was (3¹*R*)-**3R** and the second was (3¹*S*)-**3S**. Moreover, each HPLC fraction separated from **3d** was demetallated to give epimerically pure **2d**. In comparing the observed ¹H-NMR signals of the produced **2d** with the corresponding reported data,³ metal-free derivatives from the first and second bands were assigned to **2dR** and **2dS**, respectively.

Visible Spectra of Epimeric Zinc Chlorins

In a diluted dichloromethane solution (*ca.* 10 μM) of zinc chlorins **3** except **3bR** and **3cR**, all the visible absorption bands were sharp (see Fig. 1) and the widths of the Q_y band were typically about 400 cm⁻¹. Compared with previous results,⁵ the visible spectra indicated that these compounds were monomeric in the solution. In **3bR** and **3cR**, a broad band appeared in the red side of the major monomeric Q_y band (see Fig. 2). The new band was ascribed to a small aggregate, probably a dimer. In zinc fluoro- and chlorochlorins, such a shoulder was clearly observed. The electron-withdrawing substituents at the 20-position would increase the coordination ability of the central zinc¹¹ so that a dimer species was formed even in a diluted dichloromethane solution. It is of interest that the (3¹*R*)-epimers **3bR** and **3cR** more easily aggregated to give such a dimer species than the corresponding (3¹*S*)-epimers (**3bS** and **3cS**). The diastereomeric control was

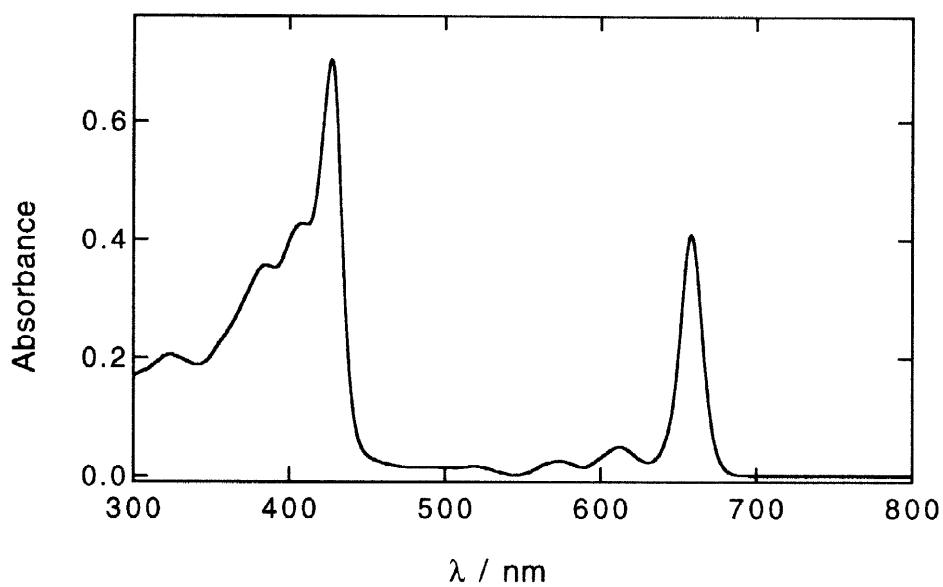
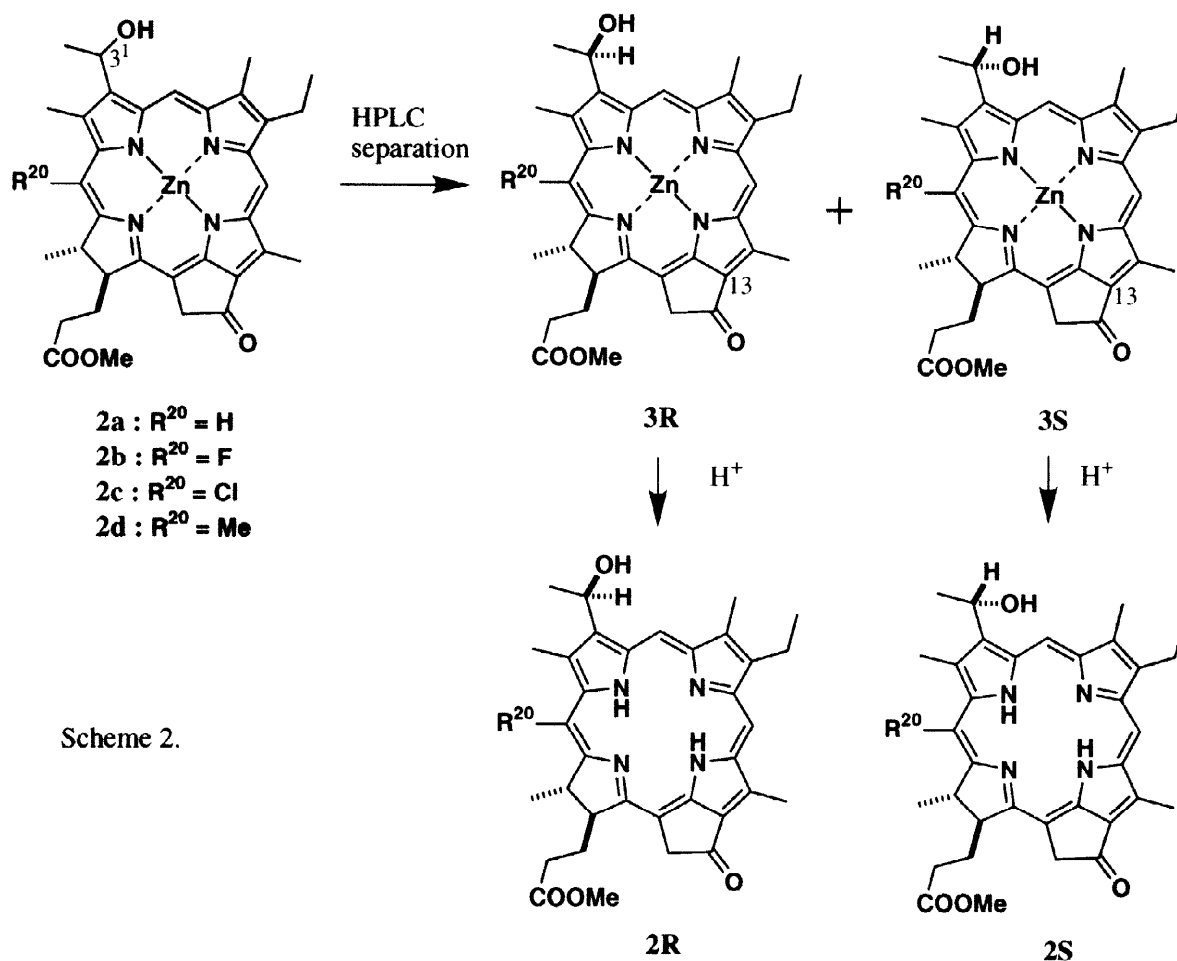


Fig. 1. UV-visible spectrum of zinc methyl 3¹S-bacteriopheophorbide-c (**3dS**) in dichloromethane (ca. 10 μ M).

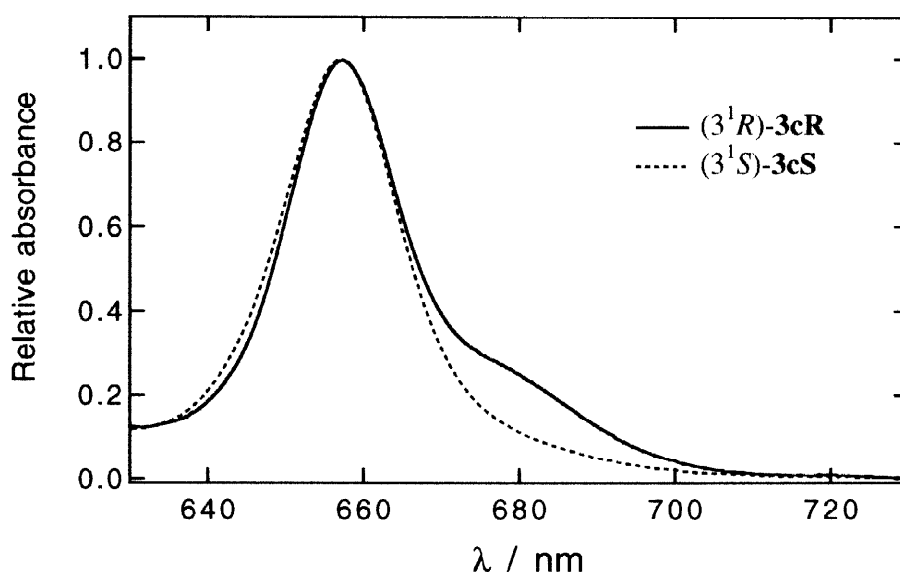


Fig. 2. Visible spectra of zinc methyl 20-chlorobacteriopheophorbide-*d* (**3cR** / **3cS**) in dichloromethane (*ca.* 10 μ M), normalized at Q_y peak.

consistent with our previous results in **3aR/S**.^{4a} In tetrahydrofuran (THF), all the zinc chlorins **3** gave sharp visible bands and were solvated with THF to give monomeric species. The FT-IR spectra showed that a THF molecule coordinated with the central zinc and another hydrogen-bonded with the 3¹-hydroxyl group⁵ (data not shown).

In monomeric species, both the epimers **3R/S** gave the same visible spectra and the Q_y peak was shifted in the order, **3a** (20-H) < **3b** (20-F) < **3c** (20-Cl) \approx **3d** (20-Me) (see Table 1). The shift was ascribed to the steric effect at the 20-substituent and a similar shift was observed in the analogous system.⁶ The molecular modeling (PM3/MM+ calculations⁶) indicated that the bulkiness of the 20-substituent distorted the chlorin π -plane, which induced red-shift of visible bands.

Table 1. Q_y maxima of epimeric zinc chlorins **3** (*ca.* 10 μ M)

	R^{20}	$\lambda_{\max} / \text{nm}$	
		CH_2Cl_2	1% (v/v) CH_2Cl_2 – cyclohexane ^a
3aR	H	648	703 [— , 705]
3aS	H	648	645, 698 [693, 706]
3bR	F	652, 672 (sh)	708 [— , 708]
3bS	F	652	647 (sh), 706 [— , 706]
3cR	Cl	658, 682 (sh)	736 [721, 743]
3cS	Cl	658	653 (sh), 716 [717, —]
3dR	Me	658	736 [— , 740]
3dS	Me	658	654, 720 [718, 732]

^a Values in brackets show negative peaks in the second derivatives at the region of oligomeric Q_y bands.

In 1% (v/v) dichloromethane–cyclohexane, all the zinc complexes **3** gave broad and red-shifted absorption bands compared with the monomeric bands described above (see Fig. 3). The red-shifted Q_y peak was higher in intensity than the corresponding Soret peak, while the Q_y peak of monomeric species was lower than the monomeric Soret peak. The visible bands observed in non-polar organic solvents are characteristic of oligomeric **3** in comparison with other reported spectra.⁵ The spectra of oligomeric (3^1R)-epimers **3R** were different from those of oligomeric (3^1S)-epimers **3S**; diastereomeric control was operated in the oligomerization of **3**. The Q_y peak of the oligomer in **3R** was more red-shifted than that in **3S**.¹⁴ The second derivative of visible spectra indicated that oligomeric Q_y peaks consisted of several components. The major component of oligomeric **3R** absorbed longer wavelengths than that of oligomeric **3S**. In the visible spectra of **3R**, monomeric species could hardly be observed around 650 nm but **3S** gave a mixture of monomeric and oligomeric species. These results indicated that (3^1R)-epimers in the non-polar organic solvents self-aggregated more tightly to give longer wavelength absorbing oligomers than (3^1S)-epimers.

The oligomerization was achieved by dilution of a concentrated dichloromethane solution (ca. 1 mM) of **3** with excess cyclohexane. In such a high concentration of the dichloromethane solution, all the zinc chlorins **3** partly self-aggregated to give several small oligomers; typically, 1.4 mM dichloromethane solution of **3dR** or **3dS** had a new 699-nm absorption peak or 684-nm shoulder, respectively. The presence of these different aggregative species in the initial concentrated solution before dilution might lead to a different oligomerization in each 3^1 -epimer, although this was ruled out by the following experiments. Addition of 0.5% (v/v) THF to the concentrated dichloromethane solution of **3** changed the visible spectra to completely monomeric sharp ones. Dilution of such a mixed solution including an exclusively monomer species with cyclohexane gave almost the same spectra as shown in Fig. 3. The results supported that oligomerization processes of each epimer **3R/S** in non-polar organic solvents were different as were the oligomerization products, which led to the different visible spectra in oligomeric **3R/S**. In all the oligomers of **3**, the local structure is the same and built-up mainly by $13-C=O\cdots H(3-CHMe)O\cdots Zn$ and π - π interaction of the chlorin chromophores reported so far.^{4a,5,6} The size and/or the orientation of each component in the oligomers is dependent on the 3^1 -configuration of the monomer and affects the supramolecular structures.

In the non-polar organic solution of unsubstituted and methylated (3^1S)-epimers **3aS** and **3dS**, monomeric peaks were clearly observed around the 650-nm region and **3bS** and **3cS** had less pronounced shoulders ascribable to the monomeric Q_y band. Zinc fluoro- and chlorochlorins aggregated more strongly than unsubstituted and methylated zinc chlorins. The electronic effect at the 20-substituent (*vide supra*) also operated in the oligomerization. Both the Q_y peaks of oligomer in **3R** and **3S** were shifted in the same order, **3a** < **3b** < **3c** \approx **3d** as that of monomer. Steric bulkiness around the 20-position did not disturb the oligomerization.

Visible and CD Spectra of Epimeric Mixtures

A species of green non-sulfur bacteria, *Chloroflexus aurantiacus*, has several homologues of BChl-*c* as major antenna pigments in chlorosomes. The BChls-*c* consist of a mixture of (3^1R)- and (3^1S)-epimers (2:1); this prompted us to examine the properties in self-aggregates of 3^1 -epimeric mixtures of the synthetic zinc chlorins **3**. A mixture of (3^1R)-**3dR** and (3^1S)-**3dS** ($R^{20}=Me$) at several ratios was dissolved in 0.5% (v/v) THF – dichloromethane to give a dark blue solution (ca. 1 mM) of only monomeric **3d** with a 660-nm absorption peak. The solution was diluted 100-fold with cyclohexane to make a green solution (ca. 10 μ M).

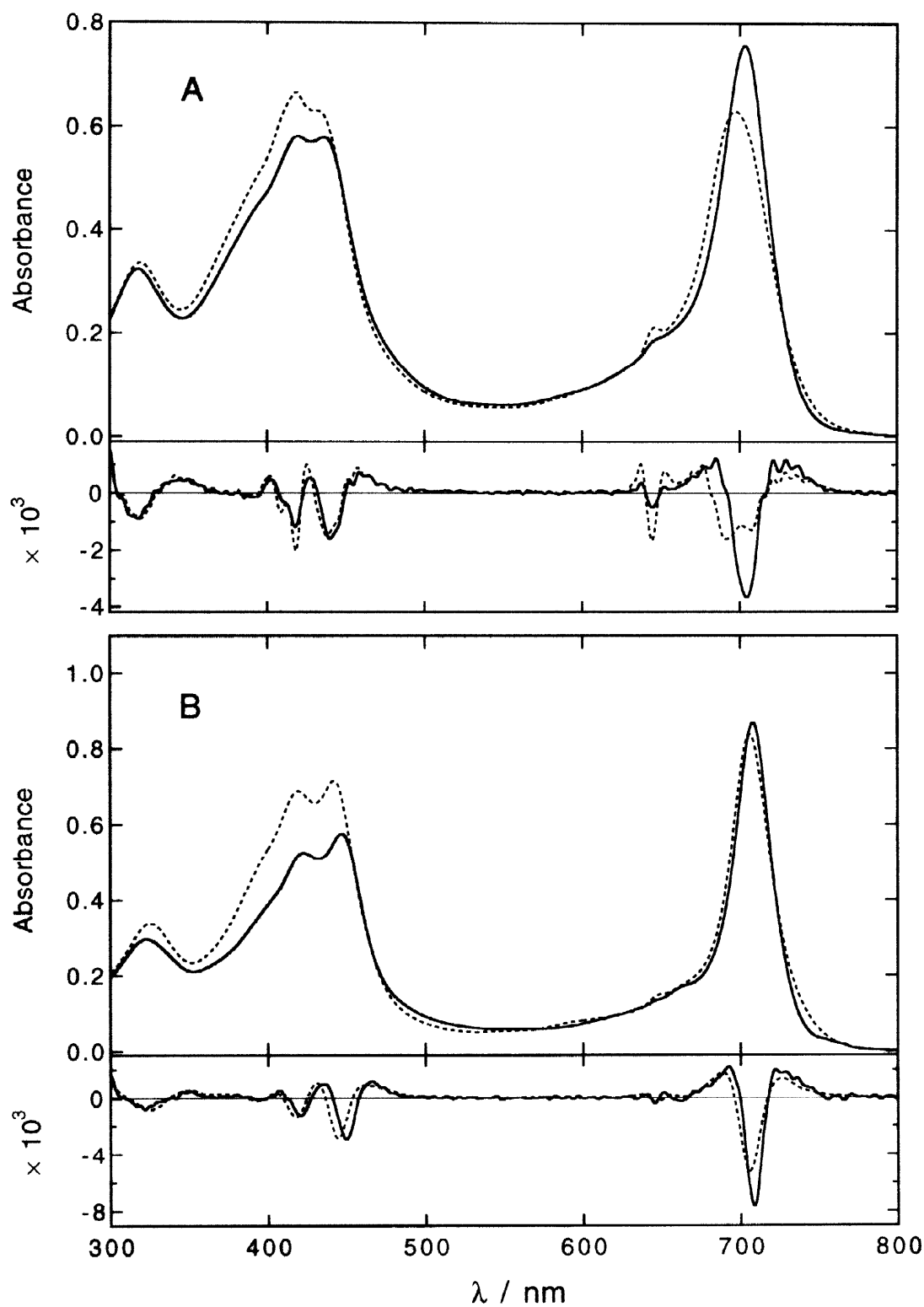


Fig. 3. UV-visible spectra and the second derivatives of epimerically pure **3** in 1% (v/v) CH_2Cl_2 - cyclohexane. —, (3^1R)-epimer **3R**; ----, (3^1S)-epimer **3S**.
A, **3a** ($\text{R}^{20}=\text{H}$); B, **3b** ($\text{R}^{20}=\text{F}$); C, **3c** ($\text{R}^{20}=\text{Cl}$); D, **3d** ($\text{R}^{20}=\text{Me}$).

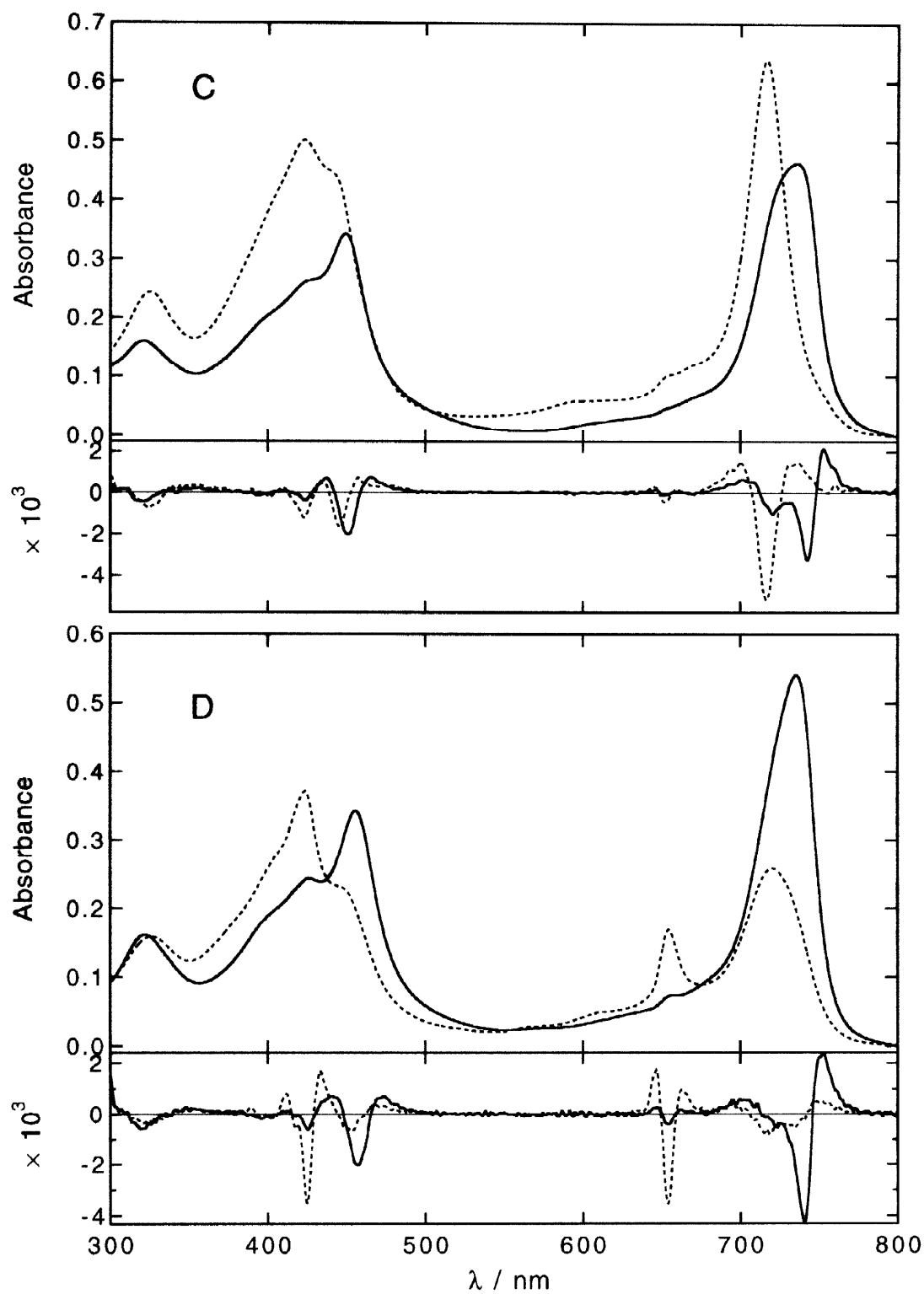


Fig. 3 (continued). UV-visible spectra and the second derivatives of epimerically pure **3** in 1% (v/v) CH_2Cl_2 – cyclohexane. —, (3^1R) -epimer **3R**; ·····, (3^1S) -epimer **3S**. A, **3a** ($R^{20} = \text{H}$); B, **3b** ($R^{20} = \text{F}$); C, **3c** ($R^{20} = \text{Cl}$); D, **3d** ($R^{20} = \text{Me}$).

In 0.005% (v/v) THF–1% (v/v) dichloromethane–cyclohexane, **3d** self-aggregated to form oligomers absorbing above 700-nm wavelengths while the monomeric species ($\lambda_{\text{max}}=654$ nm) appeared as a minor portion (see Fig. 4). As the ratio of **3dS**/**3dR** increased, the monomer peaks enhanced concomitantly with decrease of the oligomer peaks ($\lambda_{\text{max}}=715$ –740 nm). The (3^1S)-epimer **3dS** reduced the oligomerization of epimeric mixtures of **3d** as well as that of the epimerically pure sample discussed above. Moreover, the oligomer peaks were blue-shifted as the ratio of **3dS**/**3dR** increased. The second derivatives of the visible spectra in the region of Q_y band clearly indicated that a longer wavelength absorbing 740-nm component gradually changed to a shorter wavelength absorbing 718-nm component as the content of **3dS** increased in the epimeric mixture (see Fig. 5).

The CD spectra of **3dR** + **3dS** in the non-polar organic solvents are shown in Fig. 6. Both epimerically pure samples gave large CD peaks at the region of the red-shifted bands. In **3dR**, a reversed S-shaped band was observed with a minor dip at the shorter wavelengths, while the Cotton effect in **3dS** gave an exclusively similar reversed S-shape at a slightly blue-shifted region. Admixing an 3^1 -epimer before dilution greatly decreased the intensity and slightly affected the shape. The order of the supramolecular structures was distorted as the ratio of a minor epimer increased (**3dR**/**3dS** = 1/0 \rightarrow 1/1 or 0/1 \rightarrow 1/1). (3^1S)-**3dS** as an admixing epimer affected the CD spectra more than (3^1R)-**3dR**. It is interesting that the oligomers of 2:1 – 1:2 mixtures of **3dR** and **3dS** gave smaller Cotton effects although they have similar visible spectra to oligomers of epimerically pure **3dS**. These results indicated that supramolecular structures of the oligomeric **3d** were dependent upon the 3^1 -epimerical purity; **3dR**, **3dR** + **3dS** and **3dS** self-aggregated in the non-polar organic solvents to form slightly different supramolecules with the same local structure ($13\text{-C=O}\cdots\text{H(3-CHMe)O}\cdots\text{Zn}$ and π - π interaction).

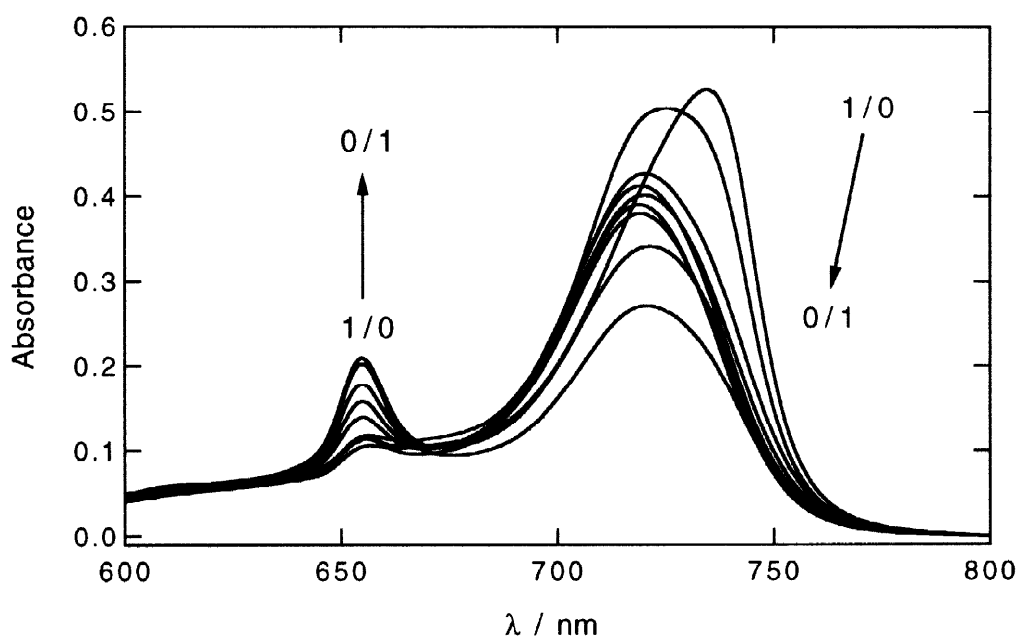


Fig. 4. Visible spectra of mixtures of (3^1R)-**3dR** and (3^1S)-**3dS** in 0.005% (v/v) – THF – 1% (v/v) CH_2Cl_2 – cyclohexane (ca. 10 μM).
3dR/**3dS** = 1/0, 12/1, 5/1, 2/1, 1/1, 1/2, 1/5, 1/12, 0/1.

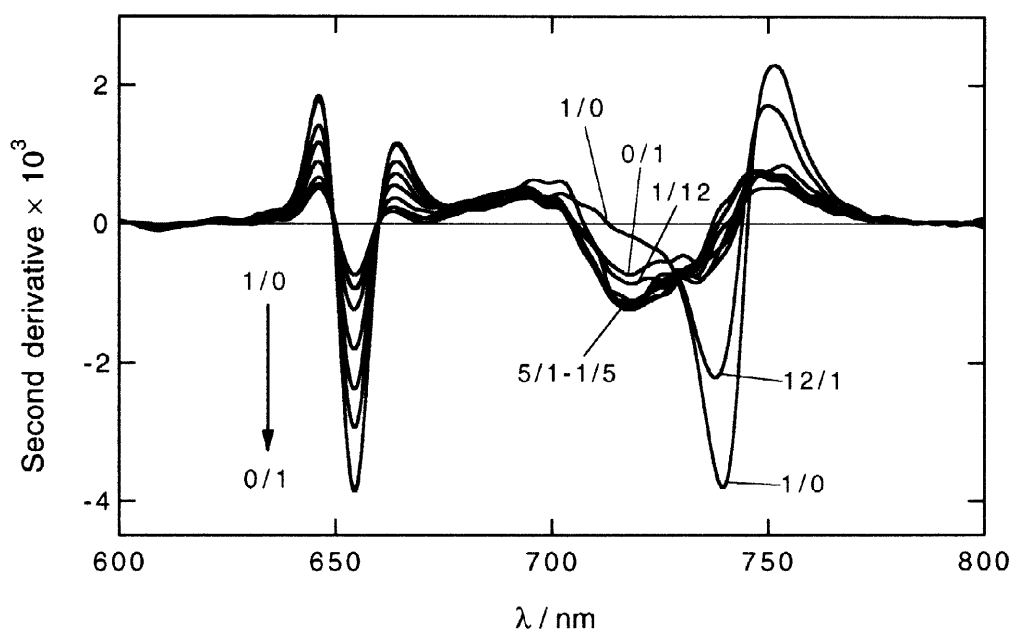


Fig. 5. Second derivatives of visible spectra of **3dR** + **3dS** mixtures in 0.005% (v/v) THF – 1% (v/v) CH_2Cl_2 – cyclohexane (ca. 10 μM).
3dR/3dS = 1/0, 12/1, 5/1, 2/1, 1/1, 1/2, 1/5, 1/12, 0/1.

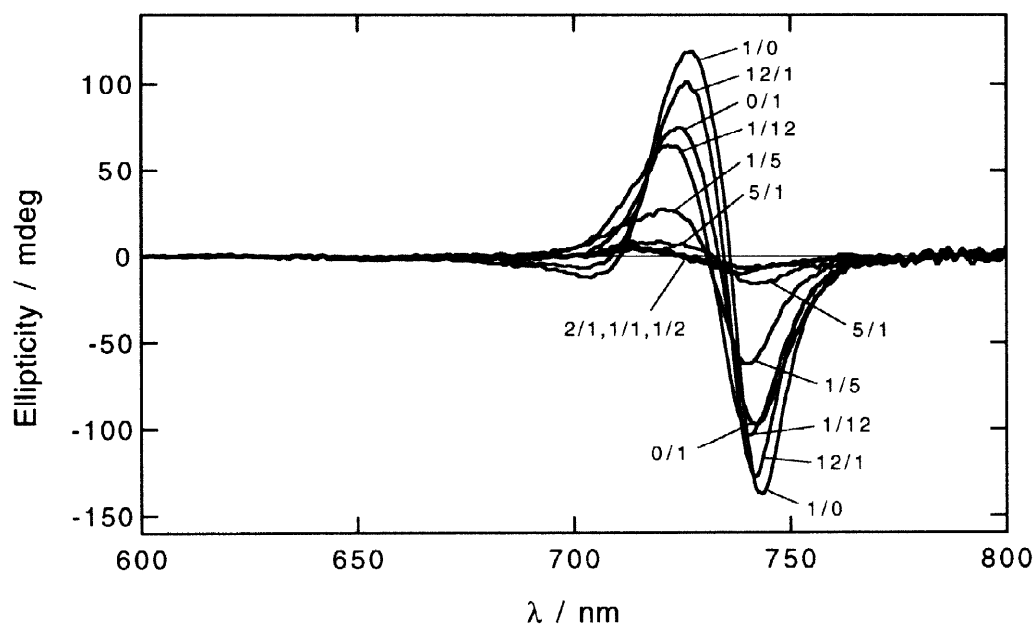


Fig. 6. CD spectra of **3dR** + **3dS** mixtures in 0.005% (v/v) THF – 1% (v/v) CH_2Cl_2 – cyclohexane (ca. 10 μM).
3dR/3dS = 1/0, 12/1, 5/1, 2/1, 1/1, 1/2, 1/5, 1/12, 0/1.

Comparison of *in vitro* Self-aggregates of Synthetic Zinc Chlorins with *in vivo* BChl-*c* Aggregate

Natural chlorosomes isolated from *Chloroflexus aurantiacus* in an aqueous buffer solution has a 741-nm peak as the red-shifted and broadened Q_y absorption and large reversed S-shape CD bands at the region with a minor negative peak at lower wavelengths (dotted lines of Fig. 7). The visible spectrum was more sharp and red-shifted than that of self-aggregates of **3dR/3dS** = 2/1 in the non-polar organic solvents (λ_{max} =720 nm in the broken line of Fig. 7A). The CD spectrum of chlorosomes was red-shifted to that of *in vitro* aggregates of the mixture as well. Moreover, the relative intensity was 4-fold higher than that of the spontaneous aggregates. These results indicated a difference in supramolecular structures between natural chlorosomes and the spontaneous self-aggregates of **3dR/3dS** = 2/1. The large Cotton effect in chlorosomes showed the orderly form of the self-aggregates of (3¹*R*)- and (3¹*S*)-BChls-*c* = 2/1 in chlorosomes. Rapid and efficient energy transfer in the chlorosomal aggregates¹² supported the regular self-assemblies. Self-aggregates of zinc (3¹*R*)- and (3¹*S*)-bacteriopheophytins-*c* (= 2/1) with long chains at the ester¹³ gave small CD peaks in the non-polar organic solvents (data not shown). Substitution of the alkyl chain on the 17-propionate did not much affect the CD intensity in the spontaneous self-aggregates of the epimeric mixtures. Moreover, Miller and his colleagues¹⁵ reported that aqueous aggregates of BChls-*c* (3¹*R/S* = 2/1) prepared by diluting a methanol solution of chloroform/methanol extracts from *Chloroflexus aurantiacus* with aqueous buffer showed 8-fold smaller Cotton effect than the intact chlorosomes. The reported suppression was consistent with the present results.

Initially self-aggregates of **3dR** and **3dS** were separately prepared in the non-polar organic solvents and then the solutions of the aggregates were mixed at a 2:1 ratio. The mixed solution after aggregation of the epimerically pure samples gave a sharper and red-shifted visible spectrum (λ_{max} =734 nm in the solid line of Fig. 7A) than the solution of aggregation of the epimeric mixture. The former solution showed 13-fold larger CD peaks than the latter (see the solid and broken lines of Fig. 7C). Both the visible and CD spectra indicated that the mixture of **3dR** aggregates/**3dS** aggregates = 2/1 was a better model as supramolecular structures of the chlorosomal aggregates of (3¹*R*)/(3¹*S*)-BChls-*c* = 2/1 than the aggregates of mixed **3dR/3dS** = 2/1. The visible spectrum of the mixture of the separated aggregates was superimposed to the sum of each spectrum (2:1) as well as the CD spectrum. The mixed solution after aggregation consisted of a mixture of separated aggregates, not random self-aggregates of the epimeric mixtures accumulated by the spontaneous aggregation of the mixtures. It can therefore be concluded that (3¹*R*)- and (3¹*S*)-BChls-*c* self-aggregated separately to form each oligomer in the chlorosomes. It is not necessary that the chlorosomes are completely separated into two parts, (3¹*R*)- and (3¹*S*)-BChls-*c* self-aggregates. It is enough that each epimerically pure oligomer unit occupying a small domain aggregates to form chlorosomal supramolecules. The presence of two components (or states) in chlorosomes was reported by analysis of CD,^{16a,b} fluorescence anisotropy,^{16b,c} linear dichroism^{16d,e} and time-resolved emission/absorption spectra^{16e-g} as well as modeling of the visible bands,^{16h} which might support such epimerically separated aggregates as proposed here. In natural chlorosomes, BChls-*c* self-aggregate in the presence of other substances including lipids, quinones, carotenoids and peptides,¹⁷ which might control the oligomerization. *In vivo* self-aggregation proceeds much more slowly than the spontaneous aggregation in the present system. Slow oligomerization of natural BChls-*c* (3¹*R/S* = 2/1) induced the regular supramolecular structures and/or the epimerically separated assemblies.

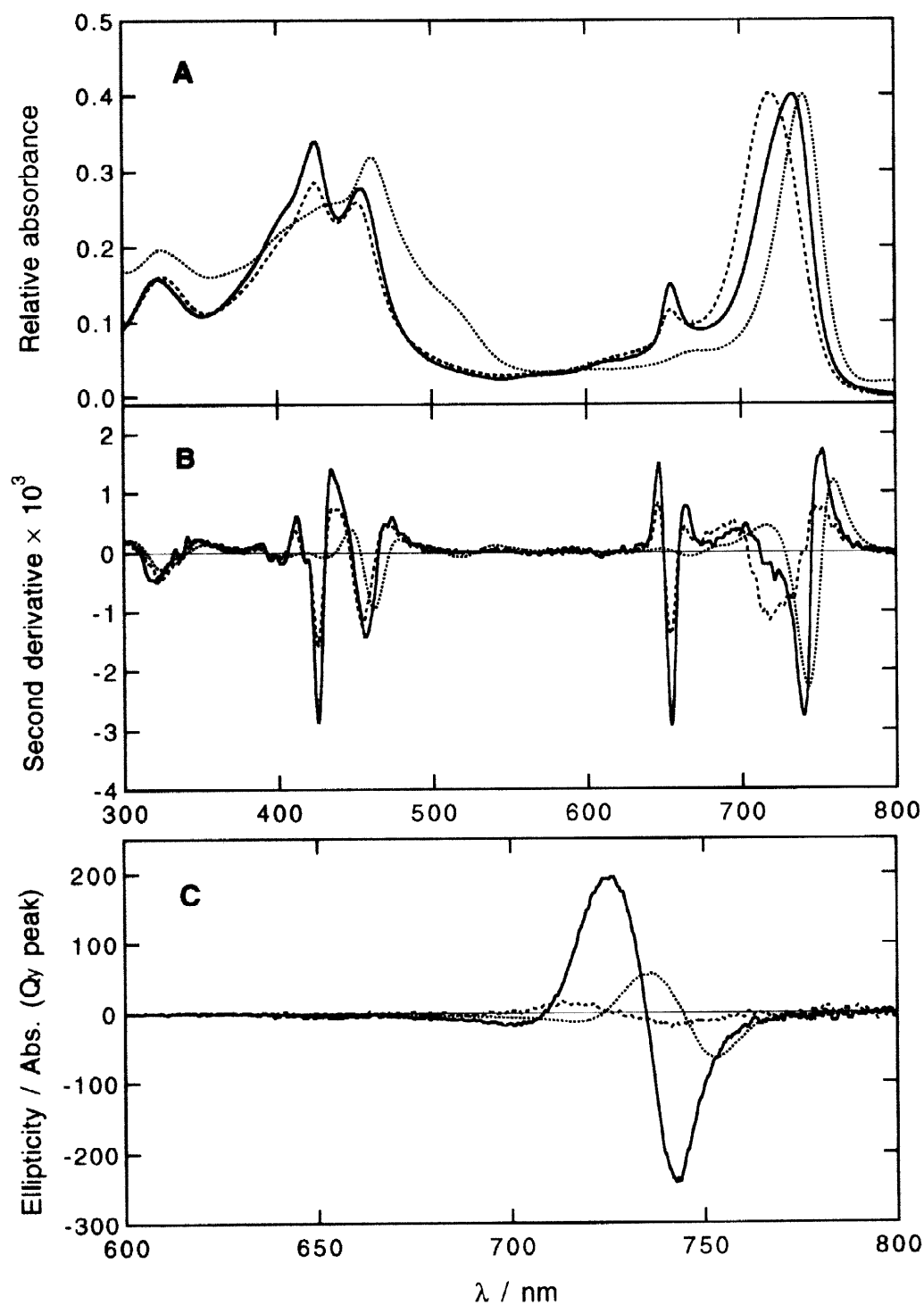


Fig. 7. UV-visible spectra normalized at Qy peak (A), second derivatives of UV-visible spectra (B) and CD spectra normalized at Qy absorption intensity (C).

....., isolated chlorosomes from *Chloroflexus aurantiacus* in 20 mM Tris-HCl buffer (pH=8);
 -.-.-, spontaneous self-aggregates of **3dR/3dS** = 2/1 in THF/CH₂Cl₂/cyclohexane = 0.005/1/99;
 —, a mixture of **3dR**-aggregates and **3dS**-aggregates (=2/1) in THF/CH₂Cl₂/cyclohexane = 0.005/1/99.

EXPERIMENTAL

Apparatus

All of the apparatus used was the same as that described in our previous report.¹⁸ Chemical shifts (δ) of ^1H -NMR spectra are expressed in parts per million relative to CHCl_3 (7.26 ppm) or CHD_2OD (3.30 ppm) as an internal reference.

Materials

Methyl pyropheophorbide-*a* (**1**) was prepared according to the procedures reported by Tamiaki and his colleagues.⁵ Toluene and CH_3CN were distilled and stored over molecular sieves 3A. THF was distilled from CaH_2 before use. Flash column chromatography (FCC) was performed with silica gel (Merck, Kieselgel 60, 9385). HPLC was performed with a packed ODS column (Gelpack GL-OP100, Hitachi Chemical Co., 6.0 $\phi \times 150$ mm or Cosmosil 5C₁₈-AR, 4.6 or 6.0 $\phi \times 250$ mm, Nacalai Tesque). Solvents for visible and CD spectra were purchased from Nacalai Tesque (Grade for UV-spectroscopy).

General

All procedures must be done in the dark!

Zinc Metallation of a Chlorin. To a saturated solution of $\text{Zn}(\text{OAc})_2 \cdot 2\text{H}_2\text{O}$ in MeOH (2 mL), a solution of a metal-free chlorin **2** (0.03 mmol) in CH_2Cl_2 (10 mL) was added and stirred at room temperature under N_2 for 2 h. Aqueous 4% NaHCO_3 (15 mL) was added to the reaction mixture, stirred for 10 min, filtered, diluted with CH_2Cl_2 , washed with H_2O and dried over Na_2SO_4 . After evaporation of the solvents, the residue was purified by FCC (eluted with 0.5–1.5% MeOH / CH_2Cl_2), recrystallization from CH_2Cl_2 / hexane and HPLC (Gelpack GL-OP100) to give a pure zinc complex **3** (3¹-epimeric mixture). Each epimer **3R/3S** was separated by a single HPLC run (Cosmosil 5C₁₈-AR); a 4.6 mm ϕ column for analytical separation (*vide supra*) and a 6.0 mm ϕ column for preparative separation (*vide infra*).

Demetallation of a Zinc Chlorin. To a solution of a zinc chlorin **3** in THF, aqueous 5% HCl was added and stirred vigorously at room temperature under N_2 for 1.5 h. The reaction mixture was poured into ice-water, extracted with CH_2Cl_2 . The organic phase was washed with aq. 4% NaHCO_3 and H_2O , dried over Na_2SO_4 , evaporated and the residue was purified by FCC (2–5% ether / CH_2Cl_2) and recrystallization from CH_2Cl_2 / hexane to give the corresponding metal-free chlorin **2**.

Methyl Bacteriopheophorbide-*d* (**2a**)

The synthetic procedures reported by Smith and his colleagues⁸ were slightly modified as follows. Methyl pyropheophorbide-*a* (**1**, 106 mg, 0.19 mmol) was dissolved in 30% hydrogen bromide in acetic acid (40 mL) and then stirred at 110 °C under N_2 for 1 h. The solution was poured into ice-water, extracted with CHCl_3 , washed with H_2O three times, and dried over Na_2SO_4 . After evaporation, the residue was dissolved in MeOH (50 mL) and to the solution was dropwise added conc. H_2SO_4 (5 mL) at 0 °C under N_2 . After 1-h stirring at room temperature, the solution was poured into ice-water, extracted with CHCl_3 and washed with H_2O three times, and dried over Na_2SO_4 . After evaporation, the residue was purified by FCC (0.2–0.4% MeOH / CH_2Cl_2) and recrystallization from CH_2Cl_2 / hexane to give 3¹-epimeric mixture of **2a** (94.2 mg, 86% yield, (3¹R) / (3¹S) = 1 / 1); black solids; mp 233–236 °C (lit.⁸ 245–247 °C); VIS (CH_2Cl_2) λ_{max} = 659 (relative intensity, 0.43), 604 (0.07), 535 (0.09), 504 (0.09), 409 (1.00), 396 (0.79), 375 (0.56) nm; ^1H -NMR

(CDCl₃) δ (*R/S*) = 9.67/69 (1H, s, 5-H), 9.49 (1H, s, 10-H), 8.51₅/50₇ (1H, s, 20-H), 6.44/42 (1H, q, *J*=7 Hz, 3-CH), 5.25/24, 5.08₅/07₉ (each 1H, d, *J*=20 Hz, 13¹-CH₂), 4.47 (1H, dq, *J*=2, 7 Hz, 18-H), 4.27 (1H, dt, *J*=8, 2 Hz, 17-H), 3.70 (2H, q, *J*=8 Hz, 8-CH₂), 3.65 (3H, s, 12-CH₃), 3.60₈/61₄ (3H, s, 17²-CO₂CH₃), 3.42/41 (3H, s, 2-CH₃), 3.25 (3H, s, 7-CH₃), 2.45–2.75, 2.20–2.35 (each 2H, m, 17-CH₂CH₂), 2.15 (3H, d, *J*=7 Hz, 3¹-CH₃), 1.80/78 (3H, d, *J*=7 Hz, 18-CH₃), 1.69 (3H, t, *J*=7 Hz, 8¹-CH₃), 0.35 (1H, br, NH), –1.80 (1H, s, NH). MS (FAB) found: *m/z* 566. Calcd for C₃₄H₃₈N₄O₄: M⁺, 566.

Methyl 20-Fluorobacteriopheophorbide-*d* (2b)

To a solution of methyl bacteriopheophorbide-*d* (2a, 45 mg, 0.079 mmol) in a minimum amount of CH₂Cl₂ (ca. 5 mL) and toluene (25 mL), a solution of *N*-fluoropyridinium triflate (190 mg, 0.77 mmol) in CH₃CN (5 mL) was added and stirred vigorously at 50 °C under N₂ for 1.5 h.⁶ The reaction mixture was washed with aq. 2% HCl, aq. 4% NaHCO₃ and aq. saturated NaCl and dried over Na₂SO₄. After evaporation, the residue was purified by FCC (2–5% ether / CH₂Cl₂) and recrystallization from CH₂Cl₂ / hexane to give the fluorinated chlorin 2b (5.1 mg, 11% yield, (3¹*R*) / (3¹*S*) = 1 / 1); black solids; mp 125–130 °C; VIS (CH₂Cl₂) λ_{\max} = 664.5 (0.37), 606 (0.05), 542.5 (0.09), 510.5 (0.09), 409.5 nm (1.00); ¹H-NMR (CDCl₃) δ (*R/S*) = 10.03/04 (1H, s, 5-H), 9.60 (1H, s, 10-H), 6.52/51 (1H, q, *J*=7 Hz, 3-CH), 5.32/31, 5.22/21 (each 1H, d, *J*=20 Hz, 13¹-CH₂), 4.77/76 (1H, q, *J*=7 Hz, 18-H), 4.30–4.38 (1H, m, 17-H), 3.73 (2H, q, *J*=7 Hz, 8-CH₂), 3.72 (3H, s, 12-CH₃), 3.59/60 (3H, s, 17²-CO₂CH₃), 3.55/56 (3H, d, *J*_{HF}=4 Hz, 2-CH₃), 3.32 (3H, s, 7-CH₃), 2.51–2.75, 2.10–2.36 (each 2H, m, 17-CH₂CH₂), 2.20/19 (3H, d, *J*=7 Hz, 3¹-CH₃), 1.76/72 (3H, t, *J*=7 Hz, 8¹-CH₃), 1.75/70 (3H, d, *J*=7 Hz, 18-CH₃), –2.88/89 (1H, s, NH¹⁹). MS (FAB) found: *m/z* 585. Calcd for C₃₄H₃₈N₄O₄F: MH⁺, 585.

Methyl 20-Chlorobacteriopheophorbide-*d* (2c)

To a solution of methyl bacteriopheophorbide-*d* (2a, 10 mg, 0.018 mmol) in THF (20 mL), a solution of NaClO₂ (1.5 mg, 3 mol) in H₂O (10 mL) was added, followed by a drop of conc. HCl and the mixture solution was stirred vigorously at room temperature under N₂ for 50 min.⁶ The reaction mixture was poured into aq. 4% NaHCO₃, extracted with CH₂Cl₂, washed with H₂O twice and dried over Na₂SO₄. After evaporation, the residue was purified by FCC (2–3% ether / CH₂Cl₂) and recrystallization from CH₂Cl₂ / hexane to give the chlorinated chlorin 2c (4.8 mg, 45% yield, (3¹*R*) / (3¹*S*) = 1 / 1); black solids; mp 130–135 °C; VIS (CH₂Cl₂) λ_{\max} = 671.5 (0.48), 613.5 (0.06), 548.5 (0.13), 516 (0.08), 412.5 nm (1.00); ¹H-NMR (CDCl₃) δ (*R/S*) = 10.02/07 (1H, s, 5-H), 9.42/39 (1H, s, 10-H), 6.48/44 (1H, q, *J*=7 Hz, 3-CH), 5.11, 5.02 (each 1H, d, *J*=20 Hz, 13¹-CH₂), 4.77/74 (1H, q, *J*=7 Hz, 18-H), 4.05–4.23 (1H, m, 17-H), 3.69 (2H, q, *J*=7 Hz, 8-CH₂), 3.63 (3H, s, 12-CH₃), 3.60/59 (3H, s, 17²-CO₂CH₃), 3.59/58 (3H, s, 2-CH₃), 3.28/27 (3H, s, 7-CH₃), 2.55–2.67, 2.20–2.45 (each 2H, m, 17-CH₂CH₂), 2.14/16 (3H, d, *J*=7 Hz, 3¹-CH₃), 1.68 (3H, t, *J*=7 Hz, 8¹-CH₃), 1.57/51 (3H, d, *J*=7 Hz, 18-CH₃), –2.12 (1H, s, NH¹⁹). MS (FAB) found: *m/z* 600. Calcd for C₃₄H₃₇N₄O₄³⁵Cl: M⁺, 600.

Methyl Bacteriopheophorbide-*c* (2d)

After complete cultivation of *Chloroflexus aurantiacus J-10-fl*,²⁰ the cultured solution (10 L) was centrifuged to give green bacteria by decantation. MeOH (200 mL) was added to the green bacteria (ca. 22 g) and the suspension was vigorously stirred for 1 h under Ar. After filtration, the residue was repeatedly extracted with MeOH / petroleum ether = 1 / 1 (200 mL), until the filtrate was colorless (three times at least).

1% (v/v) conc. HCl – brine (20 mL) was added to each filtrate and the organic phase was separated. The aqueous phase was re-extracted with several portions of diethyl ether / petroleum ether = 1 / 1 and the combined organic phases were washed with H₂O, and dried over Na₂SO₄. After evaporation, the residue was suspended in MeOH (100 mL), to which was added ice-chilled 20% (v/v) conc. H₂SO₄ – MeOH (100 mL) at 0 °C under N₂. After 1-h stirring, the solution was poured into ice-water, extracted with CH₂Cl₂, washed with H₂O several times, and dried over Na₂SO₄. After evaporation, the residue was reprecipitated from CH₂Cl₂ / hexane and washed with excess hexane to remove most orange carotenoids. The solids were purified by FCC to give carotenoids as an orange fraction (CH₂Cl₂), methyl bacteriopheophorbide-*a* as a pale red fraction (1% MeOH / CH₂Cl₂) and subsequently a major reddish black elution (2% MeOH / CH₂Cl₂). The main fraction was evaporated and recrystallized from CH₂Cl₂ / hexane to give the desired **2d**^{3,8,21} (103 mg, (3¹R) / (3¹S) = 2 / 1); black solids; mp 94–96 °C; VIS (CH₂Cl₂) λ_{max} = 670 (0.44), 612 (0.09), 551 (0.15), 520 (0.12), 482 (0.05), 414 (1.00) nm; ¹H-NMR (CDCl₃) δ (R/S) = 9.90/92 (1H, s, 5-H), 9.45 (1H, s, 10-H), 6.50/48 (1H, q, *J*=7 Hz, 3-CH), 5.21/19 (2H, s, 13¹-CH), 4.57 (1H, q, *J*=7 Hz, 18-H), 4.16 (1H, dd, *J*=3, 8 Hz, 17-H), 3.87 (3H, s, 20-CH₃), 3.70 (2H, q, *J*=8 Hz, 8-CH₂), 3.65 (3H, s, 12-CH₃), 3.58/59 (3H, s, 17²-CO₂CH₃), 3.49 (3H, s, 2-CH₃), 3.28 (3H, s, 7-CH₃), 2.45–2.60, 2.15–2.23 (each 2H, m, 17-CH₂CH₂), 2.13/15 (3H, d, *J*=7 Hz, 3¹-CH₃), 1.69 (3H, t, *J*=8 Hz, 8¹-CH₃), 1.48/46 (3H, d, *J*=7 Hz, 18-CH₃), –1.89 (1H, s, NH¹⁹). MS (FAB) found: *m/z* 580. Calcd for C₃₅H₄₀N₄O₄: M⁺, 580.

Spectral Data

Zinc Methyl Bacteriopheophorbide-*d* (3¹R/3¹S=1/1) (3a). Retention time was 5.3 min (Gelpack, MeOH, 1.5 mL / min); dark green solids; mp > 300 °C; VIS (CH₂Cl₂) λ_{max} = 648 (0.69), 603 (0.11), 555.5 (0.05), 512.5 (0.04), 422 nm (1.00); ¹H-NMR (CD₃OD) δ = 9.49, 9.46, 8.36 (each 1H, s, 5-, 10-, 20-H), 6.27 (1H, q, *J*=7 Hz, 3-CH), 5.14, 5.10 (each 1H, d, *J*=20 Hz, 13¹-CH₂), 4.44 (1H, q, *J*=7 Hz, 18-H), 4.17–4.25 (1H, m, 17-H), 3.72 (2H, q, *J*=7 Hz, 8-CH₂), 3.53, 3.34, 3.31, 3.22 (each 3H, s, 17²-CO₂CH₃, 2-, 7-, 12-CH₃), 2.55–2.70, 2.40–2.20 (each 2H, m, 17-CH₂CH₂), 2.08 (3H, d, *J*=7 Hz, 3¹-CH₃), 1.78/77 (3H, d, *J*=7 Hz, 18-CH₃), 1.69 (3H, t, *J*=7 Hz, 8¹-CH₃). MS (FAB) found: *m/z* 628. Calcd for C₃₄H₃₆N₄O₄⁶⁴Zn: M⁺, 628.

Zinc Methyl 3¹R-Bacteriopheophorbide-*d* (3aR). Retention time was 68 min (6 mmφ Cosmosil, MeOH / H₂O = 3 / 1, 1.0 mL / min); dark green solids; VIS (CH₂Cl₂) λ_{max} = 648 (0.66), 602.5 (0.11), 556.5 (0.06), 512.5 (0.05), 422 nm (1.00); ¹H-NMR (CD₃OD) δ = 9.49, 9.43, 8.36 (each 1H, s, 5-, 10-, 20-H), 6.28 (1H, q, *J*=7 Hz, 3-CH), 5.12, 4.99 (each 1H, d, *J*=20 Hz, 13¹-CH₂), 4.43 (1H, q, *J*=7 Hz, 18-H), 4.14–4.24 (1H, m, 17-H), 3.70 (2H, q, *J*=7 Hz, 8-CH₂), 3.52, 3.30, 3.29, 3.21 (each 3H, s, 17²-CO₂CH₃, 2-, 7-, 12-CH₃), 2.53–2.67, 2.18–2.41 (each 2H, m, 17-CH₂CH₂), 2.08 (3H, d, *J*=7 Hz, 3¹-CH₃), 1.77 (3H, d, *J*=7 Hz, 18-CH₃), 1.68 (3H, t, *J*=7 Hz, 8¹-CH₃). MS (CI) found: *m/z* 629. Calcd for C₃₄H₃₇N₄O₄⁶⁴Zn: MH⁺, 629.

Zinc Methyl 3¹S-Bacteriopheophorbide-*d* (3aS). Retention time was 74 min (6 mmφ Cosmosil, MeOH / H₂O = 3 / 1, 1.0 mL / min); dark green solids; VIS (CH₂Cl₂) λ_{max} = 648 (0.68), 602 (0.10), 556 (0.05), 513 (0.04), 422 nm (1.00); ¹H-NMR (CD₃OD) δ = 9.49, 9.42, 8.36 (each 1H, s, 5-, 10-, 20-H), 6.27 (1H, q, *J*=7 Hz, 3-CH), 5.12, 4.98 (each 1H, d, *J*=20 Hz, 13¹-CH₂), 4.43 (1H, q, *J*=7 Hz, 18-H), 4.13–4.23 (1H, m, 17-H), 3.70 (2H, q, *J*=7 Hz, 8-CH₂), 3.54, 3.31, 3.28, 3.21 (each 3H, s, 17²-CO₂CH₃, 2-, 7-, 12-CH₃), 2.52–2.68, 2.18–2.42 (each 2H, m, 17-CH₂CH₂), 2.08 (3H, d, *J*=7 Hz, 3¹-CH₃), 1.76 (3H, d, *J*=7

Hz, 18-CH₃), 1.67 (3H, t, $J=7$ Hz, 8¹-CH₃). MS (CI) found: m/z 629. Calcd for C₃₄H₃₇N₄O₄⁶⁴Zn: MH⁺, 629.

Zinc Methyl 20-Fluorobacteriopheophorbide-*d* (3¹R/3¹S=1/1) (3b). Retention time was 5.8 min (Gelpack, MeOH, 1.5 mL / min); dark green solids; mp > 300 °C; VIS (CH₂Cl₂) λ_{\max} = 651.5 (0.50), 606 (0.08), 567 (0.05), 522.5 (0.03), 422 nm (1.00); ¹H-NMR (CD₃OD) δ = 9.89, 9.63 (each 1H, s, 5-, 10-H), 6.36 (1H, q, $J=7$ Hz, 3-CH), 5.25, 5.16 (1H, d, $J=20$ Hz, 13¹-CH₂), 4.75 (1H, q, $J=7$ Hz, 18-H), 4.28–4.37 (each 1H, m, 17-H), 3.81 (2H, q, $J=7$ Hz, 8-CH₂), 3.64, 3.51/49, 3.31 (each 3H, s, 17²-CO₂CH₃, 7-, 12-CH₃), 3.400/3.395 (3H, d, $J_{\text{HF}}=5$ Hz, 2-CH₃), 2.51–2.71, 2.19–2.39 (each 2H, m, 17-CH₂CH₂), 2.13 (3H, d, $J=7$ Hz, 3¹-CH₃), 1.74 (3H, d, $J=7$ Hz, 18-CH₃), 1.75/73 (3H, t, $J=7$ Hz, 8¹-CH₃). MS (FAB) found: m/z 646. Calcd for C₃₄H₃₅N₄O₄F⁶⁴Zn: M⁺, 646.

Zinc Methyl 3¹R-20-Fluorobacteriopheophorbide-*d* (3bR). Retention time was 55 min (6 mm ϕ Cosmosil, MeOH / H₂O = 3 / 1, 1.2 mL / min); dark green solids; VIS (CH₂Cl₂) λ_{\max} = 651.5 (0.49), 606 (0.08), 567.5 (0.06), 522 (0.02), 422 nm (1.00); ¹H-NMR (CD₃OD) δ = 9.89, 9.62 (each 1H, s, 5-, 10-H), 6.36 (1H, q, $J=7$ Hz, 3-CH), 5.24, 5.15 (1H, d, $J=20$ Hz, 13¹-CH₂), 4.77 (1H, q, $J=7$ Hz, 18-H), 4.27–4.35 (each 1H, m, 17-H), 3.80 (2H, q, $J=7$ Hz, 8-CH₂), 3.64, 3.49, 3.31 (each 3H, s, 17²-CO₂CH₃, 7-, 12-CH₃), 3.40 (3H, d, $J_{\text{HF}}=5$ Hz, 2-CH₃), 2.53–2.70, 2.18–2.37 (each 2H, m, 17-CH₂CH₂), 2.13 (3H, d, $J=7$ Hz, 3¹-CH₃), 1.75 (3H, d, $J=7$ Hz, 18-CH₃), 1.73 (3H, t, $J=7$ Hz, 8¹-CH₃). MS (FAB) found: m/z 646. Calcd for C₃₄H₃₅N₄O₄F⁶⁴Zn: M⁺, 646.

Zinc Methyl 3¹S-20-Fluorobacteriopheophorbide-*d* (3bS). Retention time was 68 min (6 mm ϕ Cosmosil, MeOH / H₂O = 3 / 1, 1.2 mL / min); dark green solids; VIS (CH₂Cl₂) λ_{\max} = 651.5 (0.52), 605 (0.09), 567 (0.05), 524 (0.03), 422 nm (1.00); ¹H-NMR (CD₃OD) δ = 9.89, 9.62 (each 1H, s, 5-, 10-H), 6.36 (1H, q, $J=7$ Hz, 3-CH), 5.24, 5.15 (each 1H, d, $J=20$ Hz, 13¹-CH₂), 4.78 (1H, q, $J=7$ Hz, 18-H), 4.28–4.35 (1H, m, 17-H), 3.80 (2H, q, $J=7$ Hz, 8-CH₂), 3.63, 3.51, 3.31 (each 3H, s, 17²-CO₂CH₃, 7-, 12-CH₃), 3.39 (3H, d, $J_{\text{HF}}=5$ Hz, 2-CH₃), 2.52–2.71, 2.20–2.37 (each 2H, m, 17-CH₂CH₂), 2.13 (3H, d, $J=7$ Hz, 3¹-CH₃), 1.74 (3H, d, $J=7$ Hz, 18-CH₃), 1.72 (3H, t, $J=7$ Hz, 8¹-CH₃). MS (FAB) found: m/z 646. Calcd for C₃₄H₃₅N₄O₄F⁶⁴Zn: M⁺, 646.

Methyl 3¹R-20-Fluorobacteriopheophorbide-*d* (2bR). Black solids; VIS (CH₂Cl₂) λ_{\max} = 664 (0.39), 605 (0.07), 542 (0.11), 510.5 (0.10), 409.5 nm (1.00); ¹H-NMR (CDCl₃) δ = 10.03 (1H, s, 5-H), 9.60 (1H, s, 10-H), 6.52 (1H, q, $J=7$ Hz, 3-CH), 5.32, 5.22 (each 1H, d, $J=20$ Hz, 13¹-CH₂), 4.77 (1H, q, $J=7$ Hz, 18-H), 4.30–4.38 (1H, m, 17-H), 3.73 (2H, q, $J=7$ Hz, 8-CH₂), 3.72 (3H, s, 12-CH₃), 3.59 (3H, s, 17²-CO₂CH₃), 3.55 (3H, d, $J_{\text{HF}}=4$ Hz, 2-CH₃), 3.32 (3H, s, 7-CH₃), 2.51–2.75, 2.10–2.36 (each 2H, m, 17-CH₂CH₂), 2.20 (3H, d, $J=7$ Hz, 3¹-CH₃), 1.76 (3H, t, $J=7$ Hz, 8¹-CH₃), 1.75 (3H, d, $J=7$ Hz, 18-CH₃), -2.88 (1H, s, NH¹⁹). MS (FAB) found: m/z 585. Calcd for C₃₄H₃₈N₄O₄F: MH⁺, 585.

Methyl 3¹S-20-Fluorobacteriopheophorbide-*d* (2bS). Black solids; VIS (CH₂Cl₂) λ_{\max} = 665 (0.35), 607.5 (0.06), 543 (0.10), 510 (0.09), 409.5 nm (1.00); ¹H-NMR (CDCl₃) δ = 10.04 (1H, s, 5-H), 9.60 (1H, s, 10-H), 6.51 (1H, q, $J=7$ Hz, 3-CH), 5.31, 5.21 (each 1H, d, $J=20$ Hz, 13¹-CH₂), 4.76 (1H, q, $J=7$ Hz, 18-H), 4.30–4.38 (1H, m, 17-H), 3.73 (2H, q, $J=7$ Hz, 8-CH₂), 3.72 (3H, s, 12-CH₃), 3.60 (3H, s, 17²-CO₂CH₃), 3.56 (3H, d, $J_{\text{HF}}=4$ Hz, 2-CH₃), 3.32 (3H, s, 7-CH₃), 2.51–2.75, 2.10–2.36 (each 2H, m, 17-CH₂CH₂), 2.19 (3H, d, $J=7$ Hz, 3¹-CH₃), 1.72 (3H, t, $J=7$ Hz, 8¹-CH₃), 1.70 (3H, d, $J=7$ Hz, 18-CH₃), -2.89 (1H, s, NH¹⁹). MS (FAB) found: m/z 584. Calcd for C₃₄H₃₇N₄O₄F: M⁺, 584.

Zinc Methyl 20-Chlorobacteriopheophorbide-*d* (3¹R/3¹S=1/1) (3c). Retention time was 6.7 min (Gelpack, MeOH, 1.5 mL / min); dark green solids; mp > 300 °C; VIS (CH₂Cl₂) λ_{\max} = 657.5 (0.58), 613 (0.10), 573 (0.05), 425 nm (1.00); ¹H-NMR (CD₃OD)²² δ = 9.92/90, 9.57 (each 1H, s, 5-, 10-H), 6.33 (1H,

q, $J=7$ Hz, 3-CH), 5.14, 5.08 (each 1H, d, $J=20$ Hz, 13^1-CH_2), 4.15–4.19 (1H, m, 17-H), 3.77 (2H, q, $J=8$ Hz, 8-CH₂), 3.59, 3.49/48, 3.46, 3.26 (each 3H, s, $17^2\text{-CO}_2\text{CH}_3$, 2-, 7-, 12-CH₃), 2.39–2.62, 2.22–2.31 (each 2H, m, 17-CH₂CH₂), 2.12/09 (3H, d, $J=7$ Hz, 3^1-CH_3), 1.71 (3H, t, $J=8$ Hz, 8^1-CH_3), 1.62/60 (3H, d, $J=6$ Hz, 18-CH₃). MS (FAB) found: m/z 662. Calcd for $\text{C}_{34}\text{H}_{35}\text{N}_4\text{O}_4^{35}\text{Cl}^{64}\text{Zn}$: M^+ , 662.

Zinc Methyl 3^1R -20-Chlorobacteriopheophorbide-*d* (3cR). Retention time was 45 min (6 mmφ Cosmosil, MeOH / H₂O = 4 / 1, 1.2 mL / min); dark green solids; VIS (CH₂Cl₂) λ_{max} = 657 (0.57), 611.5 (0.10), 572.5 (0.07), 425 nm (1.00); $^1\text{H-NMR}$ (CD₃OD)²² δ = 9.90, 9.57 (each 1H, s, 5-, 10-H), 6.33 (1H, q, $J=7$ Hz, 3-CH), 5.14, 5.08 (each 1H, d, $J=20$ Hz, 13^1-CH_2), 4.15–4.19 (1H, m, 17-H), 3.77 (2H, q, $J=8$ Hz, 8-CH₂), 3.59, 3.49, 3.46, 3.26 (each 3H, s, $17^2\text{-CO}_2\text{CH}_3$, 2-, 7-, 12-CH₃), 2.39–2.62, 2.22–2.31 (each 2H, m, 17-CH₂CH₂), 2.12 (3H, d, $J=7$ Hz, 3^1-CH_3), 1.71 (3H, t, $J=8$ Hz, 8^1-CH_3), 1.62 (3H, d, $J=6$ Hz, 18-CH₃). MS (FAB) found: m/z 662. Calcd for $\text{C}_{34}\text{H}_{35}\text{N}_4\text{O}_4^{35}\text{Cl}^{64}\text{Zn}$: M^+ , 662.

Zinc Methyl 3^1S -20-Chlorobacteriopheophorbide-*d* (3cS). Retention time was 53 min (6 mmφ Cosmosil, MeOH / H₂O = 4 / 1, 1.2 mL / min); dark green solids; VIS (CH₂Cl₂) λ_{max} = 656.5 (0.55), 611 (0.09), 571 (0.07), 425 nm (1.00); $^1\text{H-NMR}$ (CD₃OD)²² δ = 9.92, 9.57 (each 1H, s, 5-, 10-H), 6.33 (1H, q, $J=7$ Hz, 3-CH), 5.14, 5.08 (each 1H, d, $J=20$ Hz, 13^1-CH_2), 4.15–4.19 (1H, m, 17-H), 3.77 (2H, q, $J=8$ Hz, 8-CH₂), 3.59, 3.48, 3.46, 3.26 (each 3H, s, $17^2\text{-CO}_2\text{CH}_3$, 2-, 7-, 12-CH₃), 2.39–2.62, 2.22–2.31 (each 2H, m, 17-CH₂CH₂), 2.09 (3H, d, $J=7$ Hz, 3^1-CH_3), 1.71 (3H, t, $J=8$ Hz, 8^1-CH_3), 1.60 (3H, d, $J=6$ Hz, 18-CH₃). MS (FAB) found: m/z 662. Calcd for $\text{C}_{34}\text{H}_{35}\text{N}_4\text{O}_4^{35}\text{Cl}^{64}\text{Zn}$: M^+ , 662.

Methyl 3^1R -20-Chlorobacteriopheophorbide-*d* (2cR). Black solids; VIS (CH₂Cl₂) λ_{max} = 671.5 (0.45), 613 (0.06), 548.5 (0.11), 516 (0.07), 412.5 nm (1.00); $^1\text{H-NMR}$ (CDCl₃) δ = 10.02 (1H, s, 5-H), 9.42 (1H, s, 10-H), 6.48 (1H, q, $J=7$ Hz, 3-CH), 5.11, 5.02 (each 1H, d, $J=20$ Hz, 13^1-CH_2), 4.77 (1H, q, $J=7$ Hz, 18-H), 4.05–4.23 (1H, m, 17-H), 3.69 (2H, q, $J=7$ Hz, 8-CH₂), 3.63 (3H, s, 12-CH₃), 3.60 (3H, s, $17^2\text{-CO}_2\text{CH}_3$), 3.59 (3H, s, 2-CH₃), 3.28 (3H, s, 7-CH₃), 2.55–2.67, 2.20–2.45 (each 2H, m, 17-CH₂CH₂), 2.14 (3H, d, $J=7$ Hz, 3^1-CH_3), 1.68 (3H, t, $J=7$ Hz, 8^1-CH_3), 1.57 (3H, d, $J=7$ Hz, 18-CH₃), -2.12 (1H, s, NH¹⁹). MS (FAB) found: m/z 600. Calcd for $\text{C}_{34}\text{H}_{37}\text{N}_4\text{O}_4^{35}\text{Cl}$: M^+ , 600.

Methyl 3^1S -20-Chlorobacteriopheophorbide-*d* (2cS). Black solids; VIS (CH₂Cl₂) λ_{max} = 671.5 (0.45), 612 (0.05), 548 (0.11), 516.5 (0.07), 412 nm (1.00); $^1\text{H-NMR}$ (CDCl₃) δ = 10.07 (1H, s, 5-H), 9.39 (1H, s, 10-H), 6.44 (1H, q, $J=7$ Hz, 3-CH), 5.11, 5.02 (each 1H, d, $J=20$ Hz, 13^1-CH_2), 4.74 (1H, q, $J=7$ Hz, 18-H), 4.05–4.23 (1H, m, 17-H), 3.69 (2H, q, $J=7$ Hz, 8-CH₂), 3.63 (3H, s, 12-CH₃), 3.59 (3H, s, $17^2\text{-CO}_2\text{CH}_3$), 3.58 (3H, s, 2-CH₃), 3.27 (3H, s, 7-CH₃), 2.55–2.67, 2.20–2.45 (each 2H, m, 17-CH₂CH₂), 2.16 (3H, d, $J=7$ Hz, 3^1-CH_3), 1.68 (3H, t, $J=7$ Hz, 8^1-CH_3), 1.51 (3H, d, $J=7$ Hz, 18-CH₃), -2.12 (1H, s, NH¹⁹). MS (FAB) found: m/z 600. Calcd for $\text{C}_{34}\text{H}_{37}\text{N}_4\text{O}_4^{35}\text{Cl}$: M^+ , 600.

Zinc Methyl Bacteriopheophorbide-*c* ($3^1\text{R}/3^1\text{S}=2/1$) (3d). Retention time was 6.0 min (Gelpack, MeOH, 1.5 mL / min); dark green solids; mp > 300 °C; VIS (CH₂Cl₂) λ_{max} = 658 (0.61), 612 (0.10), 574 (0.06), 427 nm (1.00); $^1\text{H-NMR}$ (CD₃OD) δ (R/S) = 9.73/71, 9.42 (each 1H, s, 5-, 10-H), 6.32 (1H, q, $J=7$ Hz, 3-CH), 5.06, 5.03 (each 1H, d, $J=20$ Hz, 13^1-CH_2), 4.53 (1H, q, $J=7$ Hz, 18-H), 4.03 (1H, dd, $J=3, 8$ Hz, 17-H), 3.74 (3H, s, 20-CH₃), 3.70 (2H, q, $J=8$ Hz, 8-CH₂), 3.53, 3.46/47, 3.33, 3.23 (each 3H, s, $17^2\text{-CO}_2\text{CH}_3$, 2-, 7-, 12-CH₃), 2.42–2.59, 2.24–2.35, 1.98–2.22 (1H+1H+2H, m, 17-CH₂CH₂), 2.07/09 (3H, d, $J=7$ Hz, 3^1-CH_3), 1.68 (3H, t, $J=8$ Hz, 8^1-CH_3), 1.44/43 (3H, d, $J=7$ Hz, 18-CH₃). MS (FAB) found: m/z 642. Calcd for $\text{C}_{35}\text{H}_{38}\text{N}_4\text{O}_4^{64}\text{Zn}$: M^+ , 642.

Zinc Methyl 3^1R -Bacteriopheophorbide-*c* (3dR). Retention time was 24 min (6 mmφ Cosmosil, MeOH / H₂O = 4 / 1, 1.5 mL / min); dark green solids; VIS (CH₂Cl₂) λ_{max} = 658 (0.63), 612 (0.10), 574 (0.06), 427 nm (1.00); $^1\text{H-NMR}$ (CD₃OD) δ = 9.67, 9.45 (each 1H, s, 5-, 10-H), 6.31 (1H, q, $J=7$ Hz, 3-

CH), 5.14, 5.11 (each 1H, d, $J=20$ Hz, 13^1-CH_2), 4.53 (1H, q, $J=7$ Hz, 18-H), 4.05 (1H, m, 17-H), 3.77 (3H, s, 20-CH₃), 3.71 (2H, q, $J=8$ Hz, 8-CH₂), 3.60, 3.48, 3.33, 3.23 (each 3H, s, $17^2\text{-CO}_2\text{CH}_3$, 2-, 7-, 12-CH₃), 2.33–2.54, 2.09–2.22 (each 2H, m, 17-CH₂CH₂), 2.06 (3H, d, $J=7$ Hz, 3^1-CH_3), 1.67 (3H, t, $J=8$ Hz, 8^1-CH_3), 1.50 (3H, d, $J=7$ Hz, 18-CH₃). MS (FAB) found: m/z 642. Calcd for $\text{C}_{35}\text{H}_{38}\text{N}_4\text{O}_4^{64}\text{Zn}$: M^+ , 642.

Zinc Methyl 3^1S -Bacteriopheophorbide-c (3dS). Retention time was 27 min (6 mm ϕ Cosmosil, MeOH / H₂O = 4 / 1, 1.5 mL / min); dark green solids; VIS (CH₂Cl₂) λ_{max} = 658 (0.61), 612 (0.10), 575 (0.04), 426 nm (1.00); $^1\text{H-NMR}$ (CD₃OD) δ = 9.66, 9.43 (each 1H, s, 5-, 10-H), 6.30 (1H, q, $J=7$ Hz, 3-CH), 5.13, 5.10 (each 1H, d, $J=20$ Hz, 13^1-CH_2), 4.50 (1H, q, $J=7$ Hz, 18-H), 4.03 (1H, m, 17-H), 3.75 (3H, s, 20-CH₃), 3.66 (2H, q, $J=8$ Hz, 8-CH₂), 3.59, 3.47, 3.31, 3.21 (each 3H, s, $17^2\text{-CO}_2\text{CH}_3$, 2-, 7-, 12-CH₃), 2.37–2.55, 2.10–2.27 (each 2H, m, 17-CH₂CH₂), 2.07 (3H, d, $J=7$ Hz, 3^1-CH_3), 1.64 (3H, t, $J=8$ Hz, 8^1-CH_3), 1.44 (3H, d, $J=7$ Hz, 18-CH₃). MS (FAB) found: m/z 642. Calcd for $\text{C}_{35}\text{H}_{38}\text{N}_4\text{O}_4^{64}\text{Zn}$: M^+ , 642.

ACKNOWLEDGMENTS

We thank Mr. Masaharu Yamada, Dainippon Ink and Chemicals for the supply of dry *Spirulina* powder, Dr. Seiji Tai and Mr. Osamu Hirai, Hitachi Chemical for the supply of polymer-based ODS Gelpack columns and Prof. Dr. Kurt Schaffner and Prof. Dr. Alfred R. Holzwarth, Max-Planck-Institut für Strahlenchemie for their helpful discussion. This work was partially supported by research grants from the Human Frontier Science Program and the Kato Memorial Bioscience Foundation, Grants-in-Aid for Scientific Research (Nos. 07454192 and 09480144) from the Ministry of Education, Science, Sports and Culture, Japan, a Sasakawa Scientific Research Grant from the Japan Science Society and a Ritsumeikan Academic Research Grant for Overseas Joint Studies. TM is grateful for his JSPS Research Fellowship for Young Scientists.

REFERENCES AND NOTES

- Recent reviews: (a) Tamiaki, H. *Coord. Chem. Rev.* **1996**, 148, 183–197; (b) Blankenship, R. E.; Olson, J. M.; Miller, M. In *Anoxygenic Photosynthetic Bacteria*; Blankenship, R. E.; Madigan, M. T.; Bauer, C. E. Eds.; Kluwer: Netherlands, 1995; pp. 399–435; (c) Olson, J. M. *Photochem. Photobiol.* **1998**, 67, 61–75.
- Tamiaki, H.; Miyata, S.; Kureishi, Y.; Tanikaga, R. *Tetrahedron* **1996**, 38, 12421–12432 and references cited therein. Very recently, two groups reported a study on *in vivo* mixed homologues with variable R⁸- and R¹²-substituents: Steensgaard, D. B.; Matsuura, K.; Cox, R. P.; Miller, M. *Photochem. Photobiol.* **1997**, 65, 129–134; Ishii, T.; Nagano, Y.; Yamamoto, T.; Uehara, K. *J. Inorg. Biochem.* **1997**, 67, 415.
- Fages, F.; Griebenow, N.; Griebenow, K.; Holzwarth, A. R.; Schaffner, K. *J. Chem. Soc., Perkin Trans. I* **1990**, 2791–2797.
- (a) Balaban, T. S.; Tamiaki, H.; Holzwarth, A. R.; Schaffner, K. *J. Phys. Chem. B* **1997**, 101, 3424–3431; (b) Balaban, T. S.; Holzwarth, A. R.; Schaffner, K. *J. Mol. Str.* **1995**, 349, 183–186; (c) Chiefari, J.; Griebenow, K.; Fages, F.; Griebenow, N.; Balaban, T. S.; Holzwarth, A. R.; Schaffner, K. *J. Phys. Chem.* **1995**, 99, 1357–1365; (d) Tamiaki, H.; Takeuchi, S.; Tanikaga, R.; Balaban, S. T.; Holzwarth, A. R.; Schaffner, K. *Chem. Lett.* **1994**, 401–402; (e) Holzwarth, A. R.; Griebenow, K.; Schaffner, K. *J.*

- Photochem. Photobiol. A: Chem.* **1992**, 65, 61–71; (f) Bobe, F. W.; Pfenning, N.; Swanson, K. L.; Smith, K. M. *Biochemistry* **1990**, 29, 4340–4348. Zhu and his colleagues denied such a diastereomeric control in the self-aggregates of magnesium complexes of **2a**: Zhu, Y.; Lin, S.; Ramakrishna, B. L.; van Noort, P. I.; Blankenship, R. E. *Photosynth. Res.* **1996**, 47, 207–218.
5. Tamiaki, H.; Amakawa, M.; Shimono, Y.; Tanikaga, R.; Holzwarth, A. R.; Schaffner, K. *Photochem. Photobiol.* **1996**, 63, 92–99.
 6. Kureishi, Y.; Tamiaki, H. *J. Porphyrins Phthalocyanines* **1998**, 2, 159–169.
 7. Tamiaki, H.; Miyatake, T.; Tanikaga, R.; Holzwarth, A. R.; Schaffner, K. *Angew. Chem. Int. Ed. Engl.* **1996**, 35, 772–774.
 8. Smith, K. M.; Bisset, G. M. F.; Bushell, M. *J. Org. Chem.* **1980**, 45, 2218–2224.
 9. Typically, a 3¹-epimeric mixture (1:1) of **2a** was eluted at 113 and 117 min with $R_s \approx 0.6$ on a single HPLC run, Cosmosil 5C₁₈-AR, 4.6 $\phi \times 250$ mm, Nacalai Tesque, CH₃OH / H₂O = 4 / 1, 1.0 mL / min.
 10. HPLC analysis showed that zinc-metallation of each epimer **2aR** / **2aS** gave epimerically pure **3aR** / **3aS** stereoselectively. No epimerization was observed during either zinc-metallation or demetallation procedure.
 11. Tamiaki, H.; Yagai, S.; Miyatake, T. in preparation.
 12. van Grondelle, R.; Dekker, J. P.; Gillbro, T.; Sundstrom, V. *Biochim. Biophys. Acta* **1994**, 1187, 1–65.
 13. Bacteriopheophytins-*c* prepared by demetallation of extracted BChls-*c* was zinc-metallated to give zinc (3¹R)- and (3¹S)-bacteriopheophytins-*c* (= 2/1) with a variety of long ester chains (cetyl, oleyl, stearyl, geranylgeranyl and phytyl).
 14. Small shoulders around 750 nm in the absorption spectra of **3S** are due to the minor oligomeric components. Several small valleys in the second derivatives are noise signals.
 15. Miller, M.; Gillbro, T.; Olson, J. M. *Photochem. Photobiol.* **1993**, 57, 98–102.
 16. (a) Griebenow, K.; Holzwarth, A. R.; van Mourik, F.; van Grondelle, R. *Biochim. Biophys. Acta*, **1991**, 1058, 194–202; (b) Ma, Y.-Z.; Cox, R. P.; Gillbro, T.; Miller, M. *Photosynth. Res.* **1996**, 47, 157–165; (c) Mimuro, M.; Hirota, M.; Nishimura, Y.; Moriyama, T.; Yamazaki, I.; Shimada, K.; Matsuura, K. *Photosynth. Res.* **1994**, 41, 181–191; (d) Matsuura, K.; Hirota, M.; Shimada, K.; Mimuro, M. *Photochem. Photobiol.* **1993**, 57, 92–97; (e) Mimuro, M.; Nishimura, Y.; Yamazaki, I.; Kobayashi, M.; Wang, Z. Y.; Nozawa, T.; Shimada, K.; Matsuura, K. *Photosynth. Res.*, **1996**, 48, 263–270; (f) Müller, M. G.; Griebenow, K.; Holzwarth, A. R. *Biochim. Biophys. Acta* **1993**, 1144, 161–169; (g) Savikhin, S.; Zhu, Y.; Blankenship, R. E.; Struve, W. S. *J. Phys. Chem.*, **1996**, 100, 17978–17980; (h) Cherepy, N. J.; Du, M.; Holzwarth, A. R.; Mathies, R. A. *J. Phys. Chem.*, **1996**, 100, 4662–4671.
 17. Takaichi, S.; Tsuji, K.; Matsuura, K.; Shimada, K. *Plant Cell Physiol.* **1995**, 36, 773–778; Frigaard, N.-U.; Takaichi, S.; Hirota, M.; Shimada, K.; Matsuura, K. *Arch. Microbiol.* **1997**, 167, 343–349.
 18. Tamiaki, H.; Kouraba, M. *Tetrahedron* **1997**, 53, 10677–10688.
 19. Another NH was too broad to be observed.
 20. Griebenow, K.; Holzwarth, A. R. *Biochim. Biophys. Acta* **1989**, 973, 235–240.
 21. Risch, N.; Brockmann, H.; Gloe, A. *Liebigs Ann. Chem.* **1979**, 408–418.
 22. 18-H around 4.82 ppm was hidden by solvent peaks.